HHS Public Access

Author manuscript

Tetrahedron Lett. Author manuscript; available in PMC 2017 December 28.

Published in final edited form as:

Tetrahedron Lett. 2016 December 28; 57(52): 5919–5923. doi:10.1016/j.tetlet.2016.11.080.

Identification of an unexpected shunt pathway product provides new insights into tirandamycin biosynthesis

Xingwang Zhang[a], **Zhong Li**[a,b], **Lei Du**[a,b], **George E. Chlipala**[c], **Patricia C. Lopez**[c], **Wei Zhang**[a], **David H. Sherman**[c,*], and **Shengying Li**[a,*]

[a]Shandong Provincial Key Laboratory of Synthetic Biology, and CAS Key Laboratory of Biofuels at Qingdao Institute of Bioenergy and Bioprocess Technology, Chinese Academy of Sciences, Qingdao, Shandong 266101, China

[b]University of Chinese Academy of Sciences, Beijing 100049, China

[c]Life Sciences Institute, Departments of Medicinal Chemistry, Chemistry, and Microbiology and Immunology, University of Michigan, Ann Arbor, MI 48109, USA

Abstract

Tirandamycin K (**7**), the first linear 7,13;9,13-diseco-tirandamycin derivative, was isolated from the *tamI* (encoding the TamI P450 monooxygenase) disruption mutant strain (*ΔtamI*) of marine *Streptomyces* sp. 307–9. Its chemical structure with relative and absolute configurations was elucidated by a combination of extensive spectroscopic analyses and biosynthetic inferences. Structural elucidation of this unusual compound provides new insights into tirandamycin biosynthesis. Moreover, examination of the biological activity of **7** confirms the essential function of the bicyclic ketal ring for antibiotic activities of tirandamycins.

Keywords

Tirandamycin; Natural product; Tetramic acid; Biosynthesis; *Streptomyces*

Tirandamycins belong to the tetramic acid family of natural products featured by a pyrrolidine-2,4-dione ring system.[1] The antibiotic streptolydigin,[2] the HIV-1 integrase inhibitor equisetin,[3] the mycotoxin cyclopiazonic acid,[4] the fungicidal dihydromaltophilin, [5] the quorum sensing related molecule 3-(1-hydroxydecylidene)- 5-(2-hydroxyethyl) pyrrolidine-2,4-dione,[6] and the anti-tumor agents aurantosides,[7] discodermides,[8] and cylindramides, [9] are among this fast growing family of secondary metabolites. Collectively, they have been attracting continuous interest due to their broad spectrum of biological activities and structural diversity.

Tirandamycins usually contain an intriguing bicyclic ketal moiety in their chemical structures, and exhibit potent antimicrobial activity by targeting bacterial RNA polymerases

*Corresponding authors. davidhs@umich.edu (D.H. Sherman), lishengying@qibebt.ac.cn (S. Li).

A. Supplementary data

Supplementary data associated with this article can be found, in the online version, at http://dx.doi.org/10.1016/j.tetlet.2016.11.080.

and hence blocking the transcriptional elongation process.[1,10] Tirandamycin A (**1**) and B (**2**) were first identified in the 1970s from a terrestrial *Streptomyces* species.[11] From 2009 to 2011, we isolated and characterized three novel congeners, including tirandamycin C (**3**),[12] D (**4**)[12] and E (**5**)[13] from marine *Streptomyces* sp. 307–9, together with the known compounds **1** and **2**. More recently, the laboratories of Shen and Ju discovered more tirandamycin derivatives (tirandamycin F–J) from *Streptomyces* sp. 17944[14,15] and *Streptomyces* sp. SCSIO 1666.[16,17] All these tirandamycins differ from one another in the extent of oxidative tailoring of the bicyclic ketal moiety (Fig. 1), which has been found to be a key determinant of potency against vancomycin-resistant *Enterococcus faecalis* (VRE).[12] This observation is consistent with the previous study[18] revealing that the streptolol ring of streptolydigin (the structural analog to bicyclic ketal of tirandamycin) is involved in a number of key contacts with RNA polymerase (the molecular target of tetramic acid antibiotics including streptolydigin and tirandamycins) determined from co-crystal structure analysis.

To date, two biosynthetic gene clusters responsible for assembly of tirandamycins have been identified independently from two different species of *Streptomyces*.[19,20] The hybrid polyketide synthase-nonribosomal peptide synthetase (PKS-NRPS) gene cluster (*tam*) is collinearly organized (Fig. 1). Based on detailed sequence analysis of individual domains using consensus sequence motifs as references, the predictions of the polyketide chain starter unit specified by the KS^Q domain, the incorporation of a malonate or methylmalonate subunit by each acyltransferase domain (AT), the stereoselectivity of the ketoreductase domain (KR) catalyzed reduction at each β-keto position, and glycine incorporation by the NRPS module, seem to be consistent with tirandamycin structures. *In vitro* characterization of two tailoring enzymes encoded by *tam*, including the P450 monooxygenase TamI,[13] and the FAD dependent dehydrogenase TamL,[13,16] has ascertained the sequential post-PKS pathway from **3**→**5**→**4**→**1**→**2** (Fig. 1). TrdE, a glycoside hydrolase family enzyme, was recently identified to be responsible for elimination of the C-11 hydroxy group from the earliest post-PKS intermediate pre-tirandamycin (**6**) via an uncertain dehydration mechanism leading to the unusual β-γ *cis* double bond (C-11=C-12) in **3**.[17] This result indicates that the unusual olefin is not a prerequisite for bicyclic ketal formation.

Previous studies of tirandamycin biosynthesis,[12,13,16,20] together with recent characterization of the streptolydigin biosynthetic system, [3] have significantly advanced understanding of the biogenesis of select tetramic acid natural products. However, a number of important biosynthetic questions remain unanswered. For example, formation of the bicyclic ketal ring represents the most intriguing issue, especially when the terpene cyclase analog TamF, and SlgX (TamF homolog in the streptolydigin gene cluster), were shown unlikely to be involved.[3,19,20] It is also unclear whether the bicyclic ring is formed before or after release of the chain elongation intermediate from the terminal TamD NRPS module.

Herein, we report the identification of a novel tirandamycin derivative – tirandamycin K (**7**) that represents the first example of linear 7,13;9,13-diseco-tirandamycin analog (Figs. 1 and 2). Structure elucidation of this compound provides new insights into the remaining biosynthetic questions noted above. Moreover, examination of the biological activity of **7**

confirms the essential function of the bicyclic ketal ring for the antibiotic activity of tirandamycins.

During the high-performance liquid chromatography (HPLC) purification of **3** from the Md2 fermentation broth of the *tamI* (encoding the TamI P450 monooxygenase) disruption mutant strain (*ΔtamI*) of *Streptomyces* sp. 307–9,[13] a minor metabolite **7** displaying a similar UV–Vis spectrum (Fig. S1) was eluted from the C18 reverse phase column. According to the comparative HPLC analysis, **7** is more polar than all tested tirandamycins except for **2** (Fig. S1).

A comparison of the 1D NMR data of **7** (Table 1) and **3**[12] demonstrated that their eastern fragments (Fig. 2) including the tetramic acid ring (C-2′–C-5′) and the backbone C-1–C-6 are highly similar to each other. In **7**, notably, the protons and carbon atoms at positions of C-2′–C-5′ and C-1–C-5 gave rise to two sets of peaks and the doubling signals disappeared from C-6, which is consistent with the well-known tautomeric behavior of tetramic acids.[1] The split signals are generated by two pairs of slowly interconverting external tautomers (**ab** and **cd**) arising from the rotation of the acyl side chain (Fig. S2). The intensity ratio between tautomer **ab** and **cd** of **7** was found to be 1.5.

When comparing the western fragment of **7** and **3**, the proton chemical shift values of **7** (*vs* **3**) for H-7 (δ_H 2.94 *vs* δ_H 3.49), H-8 (δ_H 1.15 *vs* δ_H 1.84), H-9 (δ_H 3.35 *vs* δ_H 3.90), H-10_a (δ_H 2.06 *vs* δ_H 2.33), H-10_b (δ_H 1.19 *vs* δ_H 1.96), H-11 (δ_H 3.47 *vs* δ_H 5.70), H_3-14 (δ_H 2.22 *vs* δ_H 1.38), H_3-17 (δ_H 0.91 *vs* δ_H 0.68), and H_3-18 (δ_H 1.03 *vs* δ_H 1.61) were clearly distinct from the corresponding values of **3**[12], demonstrating a different sub-structure.

Significantly, the absence of proton signals from 4 to 6 ppm indicated that **7** lacks the unique β-γ olefin (C-11=C-12) found in **3**. Instead, an additional methine signal (H-12, δ_H 2.71, m) was observed, corresponding to the proton that would be removed upon a dehydration reaction leading to the C-11=C-12 double bond in **3**.

Comparative analysis of the ^{1}H-^{1}H COSY spectra of **7** and **3** revealed similar correlation patterns (Fig. 2), suggesting that their backbone structures were closely related. Further examination of the ^{1}H-^{13}C HMBC spectrum revealed correlations from the protons H-12 (δ_H 2.71), H_3-14 (δ_H 2.21), and H_3-18 (δ_H 1.03) to a carbonyl carbon (C-13, δ_C 211.83), which strongly suggested that the bicyclic ring should not be present in **7**. Thus, we proposed that **7** is a heretofore unknown tirandamycin pathway derived metabolite, and **7** would be analogous, yet distinct from the linear intermediate **8** (Fig. 1), which is predicted based on collinear annotation of the hybrid PKS-NRPS biosynthetic assembly-line.[20]

Using the structure of **8** as a template, extensive analyses of ^{1}H and ^{13}C NMR data, and 2D correlations including ^{1}H-^{1}H COSY, HSQC, and HMBC (Table 1 and Figs. S2–S6) enabled assignment of all protons and carbons for **7** in its planar structure (Fig. 2). The most remarkable difference is the appearance of the C-9 hydroxy functionality in **7,** whereas the predicted structure **8** bears the C-8=C-9 olefin. The electrospray ionization-high resolution mass spectrometry (ESI-HRMS) data also supported the deduced chemical structure of **7**. As observed, the *m*/*z* values of 428.2040, 388.2115 (positive ion mode), and 404.2077 (negative

ion mode) should correspond to $[M-H_2O+Na]^+$ (*calc*. 428.2049), $[M-2H_2O+H]^+$ (*calc*. 388.2124) and $[M-H_2O-H]^-$ (*calc*. 404.2073) of the molecular formula of **7** ($C_{22}H_{33}NO_7$), respectively.

The relative configurations of the adjacent (1,2) or alternate (1,3) stereocenters in the acyclic carbon chain of **7** were determined using a combination of $^3J_{H,H}$ coupling constant and NOE correlation analyses for each fragment progressively (Table 1 and Figs. S7–S13).[21] First, the small coupling constant between H-6 and H-7 ($^3J_{H\text{-}6,H\text{-}7}$ = 2.5 Hz) revealed a *gauche* arrangement of the two protons in Newman projection, and NOE correlations of H-5/H-8, H-6/H-8 and H-7/H_3-16 agreed with the *erythro* configuration of C-6 and C-7 in Fisher projection, which defined the 6*R**,7*R** configurations (Fig. S8). Similarly, the large coupling constant between H-7 and H-8 ($^3J_{H\text{-}7,H\text{-}8}$ = 10.2 Hz) was consistent with an *anti* conformation in Newman projection, and NOE correlations of H-6/H-8, H-7/H-9, H-6/H-17 and H-7/H-17 revealed 7*R**,8*S** configurations (Fig. S9). The large coupling constant for H-8 and H-9 ($^3J_{H\text{-}8,\ H\text{-}9}$ = 10.4 Hz) and NOE correlations of H-7/H-9, H-8/H-10, H-9/H-17 and H-10/H-17 were consistent with 8*S**,9*S** configurations (Fig. S10). As to the 1,3 alternate stereocenter from C-9 to C-11, the two fragments of C-9—C-10 and C-10–C-11 were deduced separately with the same logic. The small coupling constant of $^3J_{H\text{-}9,H\text{-}\ 10a}$ (3.7 Hz) and the large value of $^3J_{H\text{-}9,H\text{-}10b}$ (10.2 Hz) revealed the *gauche* and *anti* arrangement for H-9/H-10a and H-9/H-10b in Newman projections (Fig. S11), respectively. The NOE correlation of H-8/H-10a, and H-9/H-11 revealed 9*S**,10a-*proR** configurations. Again, the small coupling constants between H-10a and H-11 ($^3J_{H\text{-}10a,H\text{-}11}$ = 1.9 Hz) and the large value for $H\text{-}10_b$ and H-11 ($^3J_{H\text{-}10b,H\text{-}11}$ = 10.0 Hz), together with the NOE correlations of H-9/H-11, H-10a/H-12, and H-10b/H12 revealed 10a-*proR**,11*R** configurations (Fig. S12). Finally, the large coupling constant value of $^3J_{H\text{-}11,H\text{-}12}$ (10.1 Hz) and NOE correlations between H-10a and H_3-18 confirmed 11*R**,12*R** configurations (Fig. S13). The sum of these analyses established relative configurations of 6*R**, 7*R**, 8*S**, 9*S**, 11*R**, 12*R** for **7**. Based upon the absolute configuration of **2** (6*R*, 7*R*, 8*S*) determined from a crystal structure,[22] we conclude that **7** takes the absolute configuration of 6*R*, 7*R*, 8*S*, 9*S*, 11*R*, 12*R* (Fig. 1).

The new tirandamycin derivative **7** was isolated from the *Streptomyces* sp. 307–9 *ΔtamI* strain with a yield of approximately 0.9 mg/L. To address whether its production is associated with the absence of *tamI*, we re-visited the metabolic profile of the wild type *Streptomyces* sp. 307–9 strain and found **7** was also produced, albeit in a significantly lower yield than the *ΔtamI* strain (data not shown).

Complete characterization of the structure of **7**, the first identified linear tirandamycin derivative, enabled the determination of the stereochemistry at C-12, and allowed the unreduced keto group at C-13 (due to the putatively inactive KR domain in module 1) to be firstly observed, which is essential for formation of the bicyclic ring. The fact that **7** was released by the final NRPS TamD module strongly suggests that the chain release machinery does not require formation of the bicyclic ring. However, the possibility that the bicyclic ketal ring is formed prior to the chain release cannot be excluded. In addition, it is unclear if the formation of aberrant intermediate **7** is related to the type II thioesterase (TE) TamB

presumably with proofreading activity[20] or the conserved hypothetical protein TamC (Fig. 1).

Compared to the structure of **8** predicted from the architecture of Tam PKS-NRPS assembly, **7** retains the C-9 hydroxyl group assumed to be removed by the dehydratase domain in module 3 (DH_3). Therefore, it is likely that DH_3 is skipped during biosynthesis of **7**. More surprisingly, the stereochemistry of the C-9 (9*S* or 9"*S*") and the C-11 (11*R* or 11"*S*") alcohol in **7** contradicts the B-type KR_3 and the B-type KR_2 (Fig. 1) that are predicted to establish the 9"*R*" (9*R*) and 11"*R*" (11*S*) stereochemistry[20] (the quotation marks denote a deviation from the classical *RS* system defined by Keatinge-Clay et al.[23]) based on the presence of LDD motif.[24] Interestingly, this abnormal 11*R* configuration in **7** was also seen in **6** (Fig. 1).[17] These inconsistencies point to modules 3 and 2, suggesting that atypical events might occur during these two rounds of polyketide elongation and processing. This also leads to re-consideration of a previously proposed mechanism for bicyclic ketal ring formation in tirandamycin[19] (and streptolydigin[3,25]). Specifically, the 9*R* hydroxyl group was proposed to be required for nucleophilic attack of the C-13 carbonyl carbon. The resultant hemiketalization, dehydration and attack of the C-7 OH group on the oxonium ion would generate the bicyclic ketal (Fig. 3A).[3,19] With respect to the catalyzing enzyme, it was hypothesized that DH_3 might play a significant role,[19] which if correct would require ACP_4 to swing the linear pentaketide intermediate (**9**, Fig. 3) back to DH_3 through contact between ACP_4 and DH_3. Although similar noncanonical contacts between ACP and DH domains from different modules have been previously reported in epothilone[26] and curacin[27] biosynthesis, the possibility of KR_4 providing the active site for bicyclic ring formation cannot be excluded. This hypothesis (Fig. 3A) is plausible and overrides another mechanism[20] (Fig. 3B) that we proposed before the publication of the streptolydigin biosynthetic gene cluster.[3] The retention of C-9 oxygen is in good agreement with the previous [^{13}C,^{18}O]-labeled precursor feeding study for streptolydigin,[25] showing that the C-9/C-13 bridging ether oxygen originates from the C-9/C-10 acetate unit. Due to the high similarity between the tirandamycin and streptolydigin biosynthetic gene clusters, it is likely these two pathways share a common spiroketalization mechanism. However, the presence of DH_3 indeed raises the question whether and how the C-9 alcohol escapes the dehydratase activity. Identification of **7** bearing the C-9 hydroxy clearly indicates that DH_3-catalyzed dehydration can be avoided, which provides important evidence to support the mechanism shown in Fig. 3A.

The abnormal stereochemistry of C-9 alcohol presumably installed by the B-type KR_3 with noncanonical stereoselectivity may explain why **7** escapes from the cyclization step since the incorrect configuration (9*S*) of the C-9 OH group might disfavor cyclization, thus making the pentaketide **10** skip the ring formation steps (Fig. 1). To our knowledge, there have been no previous reports of an LDD motif containing a B-type ketoreductase domain aberrantly catalyzing keto group reduction to establish the opposite stereochemistry. Exceptions have only been observed when unnatural polyketide analogs were employed prior to this study.[23,28] It could be speculated that an unusual event might occur when the triketide intermediate carried by ACP_2 binds to the catalytic groove of KR_3. Some specific active site

residues, or an atypical dynamic conformation of KR_3 may account for the "incorrect" stereochemistry.

Finally, the antibacterial activity of **7** against a select group of Gram-negative and Gram-positive strains including the *Escherichia coli* W3110 TolC disruption mutant strain, the *Staphylococcus aureus* 8325 NorA disruption mutant strain, the *S. aureus* ATCC 6538P, and the vancomycin-resistant *Enterococci* (VRE), was evaluated using **3** as a control. It was found that **7** was much less potent than **3** toward all four strains (Table 2). Together with the facts that all known bioactive tirandamycins contain a bicyclic ketal ring system, [11–17] and the analogous ketal ring in streptolydigin provides key contacts with its molecular target RNA polymerase,[18] we suggest that the bicyclic ketal moiety should be necessary for the antibacterial activity of tirandamycins.

In summary, we have identified tirandamycin K (**7**) as the first tirandamycin derivative without the bicyclic ketal system. Its discovery has motivated us to re-interrogate the tirandamycin biosynthetic pathway, which suggests that the DH_3 (or KR_4) domain is likely to be a key element for bicyclic ketal formation. To test this hypothesis, *in vitro* and *in vivo* characterization of the enzymatic functions of DH_3 and KR_4 will be required, and are currently ongoing in our laboratories.

Supplementary Material

Refer to Web version on PubMed Central for supplementary material.

Acknowledgments

This work was supported by National Natural Science Foundation of China under grant numbers of 21472204 to S.L. and 31300075 to W.Z., NIH of United States Grant R35 GM118101 to D.H.S., and the Youth Innovation Promotion Association of CAS (2015166) to W.Z. We also thank the financial support from the Applied Basic Research Programs of Science and Technology of Qingdao (14-2-4-10-jch).

References

1. Royles BJL. Chem Rev. 1995; 95:1981–2001.
2. Crum GF, Devries WH, Eble TE, Large CM, Shell JW. Antibiot Annu. 1955; 3:893–896. [PubMed: 13355382]
3. Olano C, Gómez C, Pérez M, et al. Chem Biol. 2009; 16:1031–1044. [PubMed: 19875077]
4. Holzapfel CW. Tetrahedron. 1968; 24:2101–2119. [PubMed: 5636916]
5. Graupner PR, Thornburgh S, Mathieson JT, et al. J Antibiot. 1997; 50:1014–1019. [PubMed: 9510907]
6. Lowery CA, Park J, Gloeckner C, et al. J Am Chem Soc. 2009; 131:14473–14479. [PubMed: 19807189]
7. Matsunaga S, Fusetani N, Kato Y, Hirota H. J AmChem Soc. 1991; 113:9690–9692.
8. Gunasekera SP, Gunasekera MJ. J Org Chem. 1991; 56:4830–4833.
9. Kanazawa S, Fusetani N, Matsunaga S. Tetrahedron Lett. 1993; 34:1065–1068.
10. Reusser F. Antimicrob Agents Chem. 1976; 10:618–622.
11. Meyer CE. J Antibiot. 1971; 24:2101–2119.
12. Carlson JC, Li S, Burr DA, Sherman DH. J Nat Prod. 2009; 72:2076–2079. [PubMed: 19883065]
13. Carlson JC, Li S, Gunatilleke SS, Anzai Y, Burr DA, Podust LM. Nat Chem. 2011; 3:628–633. [PubMed: 21778983]

14. Yu Z, Vodanovic-Jankovic S, Ledeboer N, et al. Org Lett. 2011; 13:2034–2037. [PubMed: 21405052]
15. Rateb ME, Yu ZG, Yan YJ, et al. J Antibiot. 2014; 67:127–132. [PubMed: 23715040]
16. Mo X, Huang H, Ma J, et al. Org Lett. 2011; 13:2212–2215. [PubMed: 21456513]
17. Mo XH, Ma JY, Huang HB, et al. J Am Chem Soc. 2012; 134:2844–2847. [PubMed: 22280373]
18. Tuske S, Sarafianos SG, Wang X, et al. Cell. 2005; 122:541–552. [PubMed: 16122422]
19. Mo XH, Wang ZW, Wang B, et al. Biochem Biophys Res Commun. 2011; 406:341–347. [PubMed: 21329667]
20. Carlson JC, Fortman JL, Anzai Y, Li S, Burr DA, Sherman DH. ChemBioChem. 2010; 11:564–572. [PubMed: 20127927]
21. Bifulco G, Dambruoso P, Gomez-Paloma L, Riccio R. Chem Rev. 2007; 107:3744–3779. [PubMed: 17649982]
22. Duchamp DJ, Branfman AR, Button AC, Rinehart KL Jr. J Am Chem Soc. 1973; 95:4077–4078. [PubMed: 4710070]
23. Keatinge-Clay AT, Stroud RM. Structure. 2006; 14:737–748. [PubMed: 16564177]
24. Caffrey P. ChemBioChem. 2003; 4:654–657. [PubMed: 12851937]
25. Chen H, Olesen SG, Harrison PHM. Org Lett. 2006; 8:5329–5332. [PubMed: 17078710]
26. Tang L, Ward S, Chung L, et al. J Am Chem Soc. 2004:126.
27. Akey DL, Razelun JR, Tehranisa J, Sherman DH, Gerwick WH, Smith JL. Structure. 2010; 18:94–105. [PubMed: 20152156]
28. Calderone CT, Bumpus SB, Kelleher NL, Walsh CT, Magarvey NA. Proc Natl Acad Sci USA. 2008; 105:12809–12814. [PubMed: 18723688]

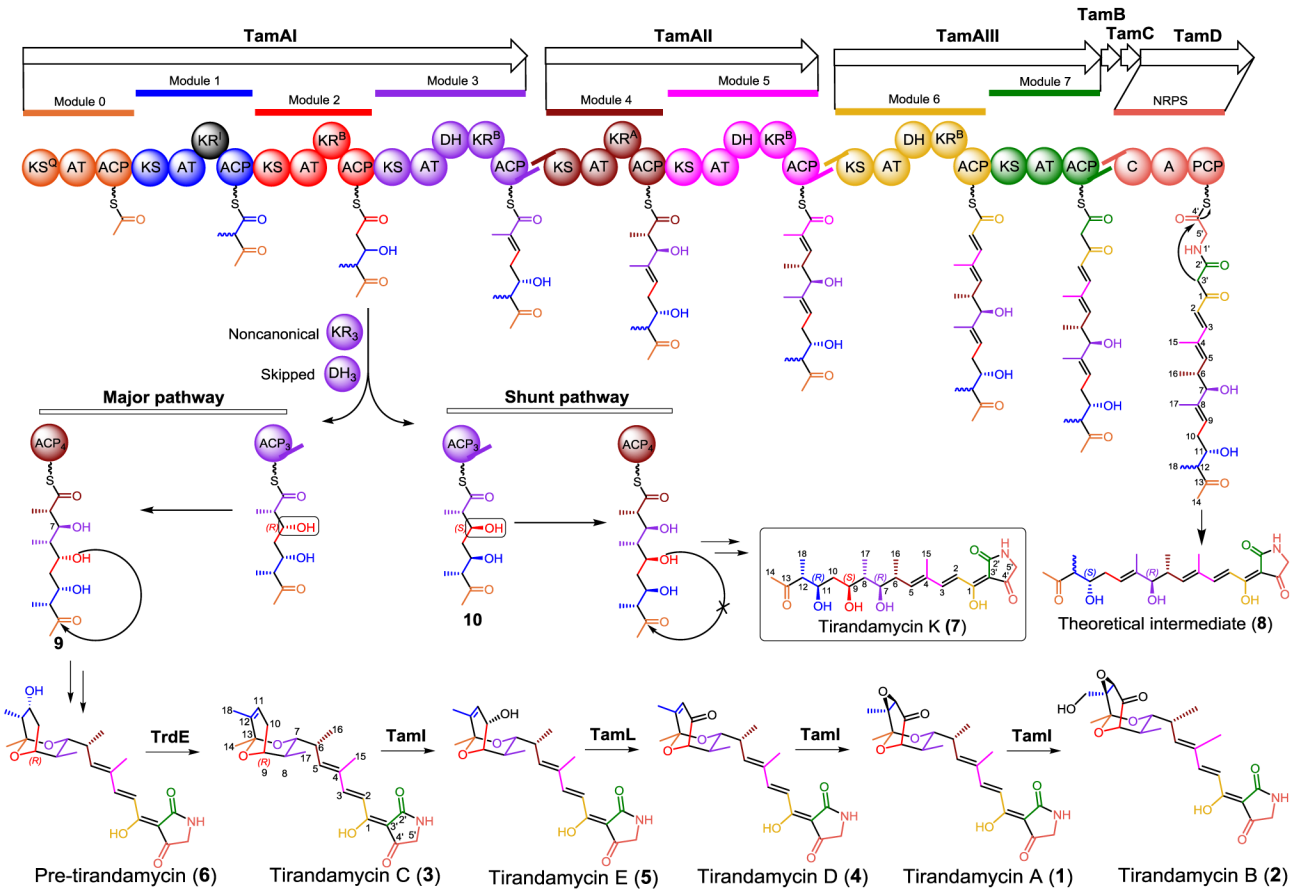

Figure 1.

Tirandamycin biosynthetic pathway (Tam) and structures of tirandamycin derivatives. The color of the individual starter or extension unit installed by the hybrid PKS-NRPS assembly-line corresponds to the installing module.

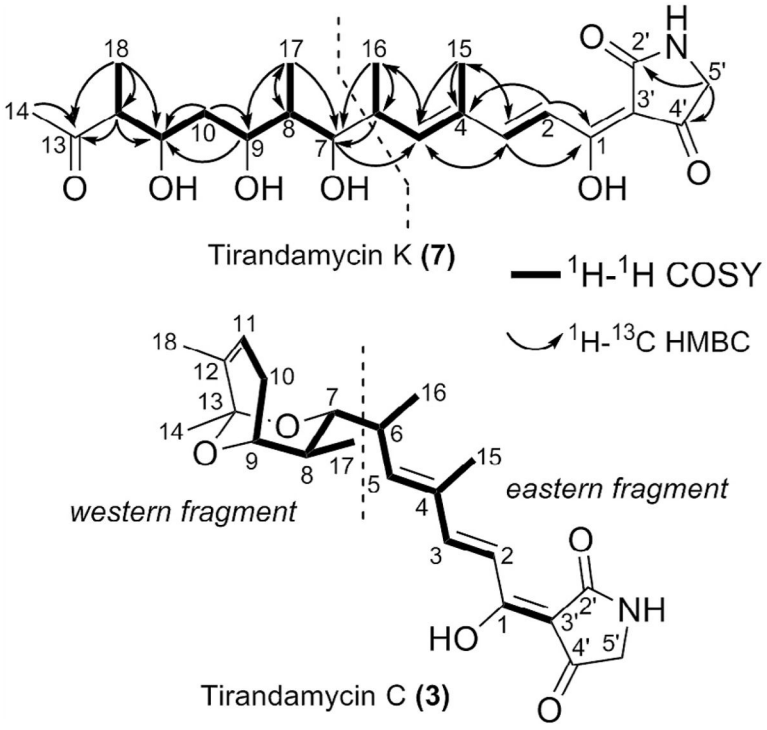

Figure 2.
^{1}H-^{1}H COSY and ^{1}H-^{13}C HMBC correlations for tirandamycin K (**7**) and C (**3**).

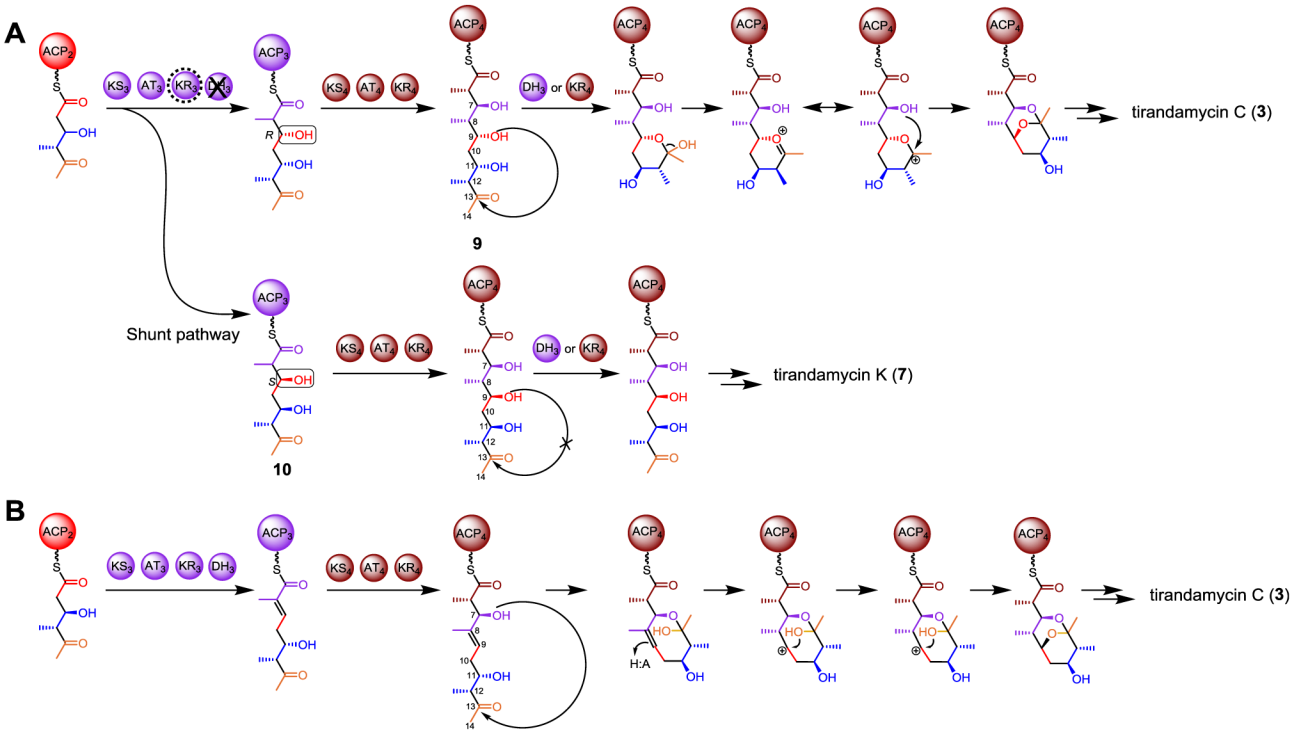

Figure 3.

Two proposed mechanisms for bicyclic ketal ring formation in tirandamycin biosynthesis. Tirandamycin K (**7**) is proposed to be a shunt pathway product in this study.

Tetrahedron Lett. Author manuscript; available in PMC 2017 December 28.

Table 1

^{1}H, ^{13}C and 2D NMR data of tirandamycin K (**7**) in $CDCl_3$.

No.	δ_C[a]	Type	δ_H, mult (*J* in Hz)[a]	^{1}H-^{1}H COSY	HMBC	NOESY
1	175.4/177.0	C				
2	116.0/115.2	CH	7.15, d (15.6)/7.14, d (15.4)	3	1, 4	15
3	150.7/152.1	CH	7.57, d (15.7)/7.64, d (15.3)	2	1, 5, 15	5
4	134.1/134.3	C				
5	146.3/147.4	CH	6.16, d (10.3)/6.21, d (10.3)	6, 15	3, 15	3, 8
6	34.8	CH	2.87, m	5, 16	7	7, 8, 15, 16, 17
7	83.9	CH	2.94, dd (10.2, 2.5)	8	5	6, 9, 11, 16, 17
8	42.1	CH	1.15, m	7, 9, 17	17	5, 6, 10a
9	73.5	CH	3.35, td (10.2, 4.6)	8, 10a, 10b	11	7, 8, 10a, 11, 17
10a	38.3	CH_2	2.06, br dd (12.3, 3.7)	9, 10b	9	8, 9, 10b, 11, 12, 18
10b			1.19, ddd (12.1, 11.7, 11.7)	9, 10a, 11	9, 11	10a, 12, 17
11	77.9	CH	3.47, td (10.0, 1.9)	10b, 12		7,[b] 9, 14, 10a, 18
12	51.6	CH	2.71, m	11, 18	11, 13	10a, 10b, 14
13	212.0	C				
14	30.3	CH_3	2.22, s		13	12, 18
15	12.2	CH_3	1.90, s	5	3, 4, 5	2, 6, 16
16	12.8	CH_3	1.04, d (7.0)	6	5, 6, 7	7, 15
17	12.4	CH_3	0.91, d (6.5)	8	7, 8, 9	6, 7, 9, 10a
18	17.9	CH_3	1.03, d (7.0)	12	11, 12, 13	10a, 11, 14
2′	176.6/175.1	C				
3′	99.8/101.9[c]	C				
4′	192.4/200.8	C				
5′	51.6/49.8	CH_2	3.97, s/3.84, s		2′, 4′	

[a] Chemical shifts of tautomers of **ab** and **cd**, respectively; 400 MHz for ^{1}H NMR and 150 MHz for ^{13}C NMR spectra.

[b] The NOESY correlation between H-11 and H-7 might be derived from conformational flexibility of the linear chain.

[c] Signals were observed in ^{13}C NMR spectrum but related HMBC correlations could not be observed.

Table 2

Biological activities of tirandamycin K (**7**) and C (**3**).

	Minimal inhibitory concentration (μM)	
	Tirandamycin K (7)	**Tirandamycin C (3)**
Escherichia coli TolC mutant W3110	100	0.78
Staphylococcus aureus ATCC 6538P	>400	12.5
Multidrug resistant *S. aureus* (MRSA)	>400	25
Vancomycin-resistant *enterococci* (VRE)	200	12.5